

## **Supplementary Material of**

Mechanisms of dissolved and labile particulate iron supply to shelf waters and phytoplankton blooms off South Georgia, Southern Ocean

Christian Schlosser, Katrin Schmidt, Alfred Aquilina, William B. Homoky, Maxi Castrillejo, Rachel A. Mills, Matthew D. Patey, Sophie Fielding, Angus Atkinson, and Eric P.

Achterberg

### **Supplementary Text**

#### **Text S1: Seawater sampling and analysis**

Water column samples were collected using trace metal clean OTE bottles deployed on a Kevlar line. The OTE bottles were transferred into the clean container where all sample handling was performed. Dissolved and total dissolvable seawater samples were acidified immediately with concentrated trace metal grade nitric acid (HNO<sub>3</sub>, UpA, Romil) to pH 1.66 (22 mmol H<sup>+</sup> L<sup>-1</sup>). Acidified seawater samples were shipped to the National Oceanography Centre Southampton and analyzed by isotope dilution (ID) and standard addition inductively coupled plasma - mass spectrometry (ICP-MS).

The preconcentration and ICP-MS analysis was adapted from the method outlined by Rapp et al. (2017). Approximately one year after collection, 12 mL of acidified seawater was transferred into 30 mL fluorinated ethylene propylene (FEP) bottles and spiked with a spike solution containing mainly the artificially enriched isotope of iron (<sup>57</sup>Fe). For the analysis of Al, and Mn a series of four standard additions were performed on every tenth sample. To obtain equimolar conditions between the spike and the natural seawater concentration, larger amounts of spike was added to the total dissolvable seawater samples. All samples were irradiated with strong ultraviolet light for 3.5 hours. Subsequently, the sample solution was

25 buffered to pH 6.4 using a 2 M ammonium acetate solution (pH9.2, Fisher Optima grade  
26 ammonia and acetic acid, glacial). Immediately after buffer addition the solution was  
27 preconcentrated using an automated system (Preplab, PS Analytical) that was equipped with  
28 a metal chelating resin (WACO) resin (Kagaya et al., 2009). Any remaining seawater salts  
29 were rinsed off using deionized water ( $> 18 \text{ M}\Omega \text{ cm}$ , MilliQ, Millipore). The metals retained  
30 on the resin were eluted using 1 mL of a 1 M sub-boiled  $\text{HNO}_3$  solution, which was collected  
31 in acid cleaned 4 mL polypropylene vials. The collected vials were placed into the auto-  
32 sampler of the ICP-MS (Element XR, Thermo).

33 The difference between the total dissolvable (TDM) and dissolved metal (DM)  
34 concentrations was used to determine the particulate concentration ( $\text{LP}_{\text{UNM}} = \text{TDM} - \text{DM}$ ). It  
35 should be noted that this particulate fraction represents the amount of Fe ( $\text{LP}_{\text{UNFe}}$ ), Al  
36 ( $\text{LP}_{\text{UNAl}}$ ), and Mn ( $\text{LP}_{\text{UNMn}}$ ) re-dissolved from particles within 1 year after the addition of  
37  $22 \text{ mmol H}^+ \text{ L}^{-1}$ . This means acid-inert minerals (e.g. zircon) and their associated trace metals  
38 likely did not contribute to the particulate metal concentration.

39 Certified seawater standards (SAFe D2 and GEOTRACES D) were preconcentrated  
40 and analyzed with each batch of samples, in order to validate our sample concentration.  
41 Values obtained by us for the certified seawater standards agreed with reported values for the  
42 GEOTRACES and the SAFe standard seawater (SAFe D2:  $0.92 \pm 0.02 \text{ nmol Fe L}^{-1}$  (certified  
43  $0.90 \pm 0.02 \text{ nmol Fe L}^{-1}$ ), GEOTRACES D:  $1.00 \pm 0.04 \text{ nmol Fe L}^{-1}$  (certified  $0.95 \pm 0.05$   
44  $\text{nmol Fe L}^{-1}$ ). The precision for replicate analyses was between 1-3%. The buffer blank was  
45  $0.056 \pm 0.016(\sigma_{\text{bl}}) \text{ nmol Fe L}^{-1}$ , and the limit of detection (3 x standard deviation of the  
46 blank) was determined as  $0.061 \pm 0.020(\sigma_{\text{bl}}) \text{ nmol Fe L}^{-1}$ .

## 47 **Test S2: Sediment and porewater sampling and analysis**

48 Sediment cores with an undisturbed sediment-seawater interface were immediately  
49 transferred to a  $\text{N}_2$ -filled glove bag in a temperature-controlled laboratory to simulate ambient

50 bottom water temperatures (approximately 4°C). Sediments were manually extruded at depth  
51 intervals of 1 or 2 cm into a polycarbonate ring, and sectioned using a polytetrafluoroethylene  
52 (PTFE) sheet that was cleaned with deionised water between each application. Porewater was  
53 separated from each sediment section by centrifugation at 9,000 g at 4°C under N<sub>2</sub> for 10  
54 minutes; the supernatant porewaters were filtered under N<sub>2</sub> through 0.2 µm cellulose nitrate  
55 syringe filters (Whatman, UK). Aliquots of each porewater sample were collected in acid-  
56 cleaned LDPE bottles (Nalgene) and acidified to pH <2 by adding 2 µL of concentrated  
57 hydrochloric acid (HCl, UpA, Romil) per 1 mL of sample; acidified samples were stored  
58 refrigerated prior to analysis at NOCS. Conjugate sediments were freeze dried on board and  
59 stored at room temperature, pending analysis at the NOCS.

60 Sub-samples (~100 mg) of the bulk, homogenized sediments were completely  
61 dissolved using hot aqua regia (HNO<sub>3</sub>+HCl) followed by hot hydrofluoric-perchloric acid  
62 (HF-HClO<sub>4</sub>) mixtures and finally diluted in 0.6M HCl as described elsewhere (Homoky et al.,  
63 2011). The acid digests were analysed by ICP-OES (Perkin Elmer Optima 4300DV).  
64 Calibration standards were matrix-matched and blank and instrument drift were monitored  
65 and corrected for by including calibration blanks and multi-element standards with each batch  
66 of 10 analyses. To ascertain the accuracy of the method certified reference material MAG-1  
67 (United States Geological Survey) was analysed with each batch of samples. The values  
68 measured in our laboratory are in close agreement with the certified values: 42.978 ± 3.155 g  
69 Fe kg<sup>-1</sup> (certified 47.600 ± 4.200 g Fe kg<sup>-1</sup>); 715 ± 9 ng Mn g<sup>-1</sup> (certified 760 ± 69 µg Mn kg<sup>-1</sup>);  
70 and 76.605 ± 2.740 g Al kg<sup>-1</sup> (certified 86.800 ± 1.600 g Al kg<sup>-1</sup>).

71 Acidified porewater samples were analysed for a suite of major and trace elements, by  
72 ICP-OES (Perkin Elmer Optima 4300 DV). Elements including Fe and Mn were measured at  
73 50-fold dilutions of the porewater sample in 0.6M HCl. Calibration standards were matrix  
74 matched and blank and instrument drift were monitored and corrected for by including

75 calibration blanks and multi-element standards for each batch of ten analyses. The instrument  
76 limits of detection (LD, 3 x standard deviation of acid blanks) were 1.25  $\mu\text{g Fe kg}^{-1}$  and 0.08  
77  $\mu\text{g Mn kg}^{-1}$ .

### 78 **Text S3: Calculation of dissolved Fe and Mn fluxes from shelf sediment porewaters**

79 The calculation of pore water Fe and Mn fluxes follows the approach of Boudreau  
80 and Scott (1978), who described the flux of pore water Mn(II) by diffusion and reaction  
81 through an oxygenated surface layer in marine sediments.

$$J = \frac{\varphi(D_s k_1)^{0.5} C_p}{\sinh((k_1/D_s)^{0.5} L)}$$

82 Where  $J$  is the flux ( $\text{g cm}^{-2} \text{s}^{-1}$ ) of Mn(II) from sediment pore water to bottom water,  
83  $L$  is the thickness (cm) of the oxygenated surface layer where Mn(II) is removed from the  
84 pore water by oxidative precipitation in the sediment, and  $C_p$  is the concentration ( $\text{g cm}^{-3}$ ) of  
85 Mn(II) in the pore water beneath  $L$  relative to the overlying bottom water. The diffusive rate  
86 constant,  $D_s$  ( $\text{cm}^2 \text{s}^{-1}$ ), is derived from sediment porosity ( $\varphi$ ), and the Mn(II) oxidation rate  
87 constant,  $k_1$  ( $\text{s}^{-1}$ ), is estimated from field studies (Boudreau and Scott, 1978). This method has  
88 more recently been adopted for the determination of pore water Fe(II) fluxes (Homoky et al.,  
89 2013; Raiswell and Anderson, 2005) using the Fe(II) oxidation kinetics of (Millero et al.,  
90 1987) to derive  $k_1$ , and has been favourably compared with incubated flux determinations  
91 from shelf sediments (Homoky et al., 2012).

92 We use measured and estimated values for scalar terms for the flux calculations that  
93 are summarised in Supplementary Table S1 to investigate the potential for pore water fluxes  
94 of Fe and Mn from sites S1, S2 and S3. Sediment porosity ( $\varphi$ ) was measured by the change in  
95 wet sediment mass after drying sliced core samples. Oxygen penetration depth ( $L$ ) was  
96 measured from a single sediment core from site S3 with a Unisense microsensor apparatus  
97 following Homoky et al. (2013), and in the absence of multiple determinations is extrapolated  
98 to each core site. Diffusion coefficients ( $D_s$ ) are derived from measurements of  $\varphi$  after

99 Boudreau and Scoot (1978). The oxidation rate constant ( $k_1$ ) for Mn(II) is also derived from  
100 Boudreau and Scoot (1978). For Fe(II),  $k_1$  is calculated from values of bottom water O<sub>2</sub>,  
101 temperature (0 °C), salinity (34) and an estimated pore water pH of 7.5 (Homoky et al.,  
102 2012), following Millero et al. (1987) (Homoky et al., 2013; Homoky et al., 2012; Raiswell  
103 and Anderson, 2005). Values of  $C_p$  are for measured data (at 0.5 and 1.5 cm depth) closest to  
104 the depth of  $L$  from each core site. Corresponding fluxes of pore water Fe (<0.1 to 44.4  $\mu\text{mol}$   
105  $\text{m}^2 \text{d}^{-1}$ ) and Mn (0.6 to 4.1  $\mu\text{mol m}^2 \text{d}^{-1}$ ) fall within the range of fluxes measured from  
106 continental margin sediments of the northeast Pacific (John et al., 2012; McManus et al.,  
107 2012) and demonstrate South Georgia shelf sediments are also likely to be an important  
108 source of Fe and Mn to the water column.

#### 109 **Text S4: Estimation of phytoplankton Fe requirements and Fe fluxes**

110 The Fe requirements of the phytoplankton community within the bloom were estimated by  
111 combining satellite derived marine net primary productivity data ( $\text{NPP} = 62 \pm 21 \text{ mmol C m}^{-2}$   
112  $\text{d}^{-1}$  (Ma et al., 2014)) with an average intracellular Fe:C ratio ( $5.2 \pm 2.8 \mu\text{mol Fe mol}^{-1} \text{C}^{-1}$   
113 (Strzepek et al., 2011)). NPP was estimated from satellite-derived information using a  
114 phytoplankton pigment absorption based model (Ma et al., 2014). The applied NPP rate  
115 corresponded to an average chlorophyll a content in the euphotic zone of  $\sim 4 \mu\text{g L}^{-1}$ . There  
116 are several literature values for Fe:C ratio estimates ranging from 6 – 14  $\mu\text{mol Fe mol}^{-1} \text{C}^{-1}$   
117 under natural non Fe-fertilized and 10 – 40  $\mu\text{mol Fe mol}^{-1} \text{C}^{-1}$  under Fe-fertilized conditions  
118 for Southern Ocean diatoms, autotrophic flagellates, and heterotrophic flagellates (Twining et  
119 al., 2004). Lab based incubation experiments using coastal phytoplankton species, such as  
120 *Dunaliella tertiolecta*, *Pyramimonas parkeae*, *Nannochloris atomus*, *Pycnococcus provasoli*,  
121 *Tetraselmis* sp., *Gymnodinium chlorophorum*, *Prorocentrum mimimum*, *Amphidinium*  
122 *carterae*, *Thoracosphaera heimii*, *Emiliana huxleyia*, *Gephyrocapsa oceanica*, *Ditylum*  
123 *brightwellii*, *Thalassiosira weissflogii*, *Nitzschia brevirostris*, and *Thalassiosira eccentric*,

124 reviled an average value of  $\sim 51 \mu\text{mol Fe mol}^{-1} \text{C}^{-1}$  (Ho et al., 2003), while Southern Ocean  
125 phytoplankton species including *Phaeocystis antarctica* (clone AA1), *Fragilariopsis*  
126 *kerguelensis*, *Thalassiosira Antarctica*, *Eucampia Antarctica*, and *Proboscia inermis* were an  
127 order of magnitude lower between 1.8 – 8.6 (Strzepek et al., 2011). Because most  
128 phytoplankton species from the Southern Ocean are very well adapted to the very low Fe  
129 water content b, we decided to apply the rather low average Fe:C ratios provided by Strzepek  
130 et al. (Strzepek et al., 2011). Even though the Fe:C ratio in the blooming region is higher, by  
131 applying this low Fe:C ratio we estimated the minimum amount of DFe that has to be  
132 supplied.

133 The vertical Fe flux ( $J_z$ ) was calculated using an approach outlined in de Jong et al.  
134 (2012). The vertical DFe flux is the sum of advective Ekman pumping (left term) and  
135 diffusion (right term).

$$J_z = w[DFe]_{BWL} + K_z \left( \frac{\delta[DFe]}{\delta z} \right)$$

136 The advective Fe flux term (left) expressed by the upwelling velocity ( $w$ ), which was set  
137 constant  $\sim 1.1 * 10^{-6} \text{ m s}^{-1}$  (de Jong et al., 2012), and the average dissolved Fe concentration  
138 ( $[DFe]_{BWL}$ ) at all stations at  $\sim 200 \text{ m}$  depth, contributed to 38% to the entire vertical Fe flux  
139 of  $0.41 \mu\text{mol m}^{-2} \text{ d}^{-1}$ . The remaining 62% are contribution of the diffusive mixing term (right)  
140 which was derived from the DFe gradient at all stations between the surface mixed layer and  
141  $\sim 200 \text{ m}$  water depth and the vertical diffusivity, set constant at  $K_z = 1 * 10^{-4} \text{ m}^{-2} \text{ s}^{-1}$ .

142 **Supplementary Tables**

143 **Table S1: Summary of pore water Fe and Mn flux parameters**

Parameter	Unit	----- Fe -----			----- Mn -----		
		S1	S2	S3	S1	S2	S3
Site		S1	S2	S3	S1	S2	S3
Pore w. conc. $C_p$	(g cm <sup>-3</sup> )	1.7E-07 to 9.6E-07	6.2E-08 to 8.6E-08	9.2E-08 to 1.7E-06	4.9E-08 to 1.3E-07	1.8E-08 to 4.0E-08	2.2E-08 to 2.8E-08
O <sub>2</sub> depth, $L$	(cm)	0.7	0.7	0.7	0.7	0.7	0.7
Porosity, $\phi$		0.76	0.76	0.84	0.76	0.76	0.84
Diff. coef., $D_s$	(cm <sup>2</sup> s <sup>-1</sup> )	2.076E-06	2.076E-06	2.461E-06	1.877E-06	1.877E-06	2.156E-06
Bottom water [O <sub>2</sub> ]	(g cm <sup>-3</sup> )	1.574E-05	1.574E-05	1.700E-05	1.00E-07	1.00E-07	1.00E-07
Pore water pH		7.5	7.5	7.5	7.5	7.5	7.5
Oxidation rate, $k_1$	(s <sup>-1</sup> )	1.574E-05	1.574E-05	1.700E-05	1.00E-07	1.00E-07	1.00E-07
Flux, $J$	(g cm <sup>3</sup> s <sup>-1</sup> )	2.2E-13 to 1.2E-12	4.3E-15 to 6.1E-15	1.6E-13 to 2.9E-12	1.0E-13 to 2.6E-13	3.6E-14 to 8.1E-14	5.8E-14 to 7.3E-14
	( $\mu$ mol m <sup>2</sup> d <sup>-1</sup> )	3.4 to 19.2	<0.1	2.5 to 44.4	1.6 to 4.1	0.6 to 1.3	0.9 to 1.1

144

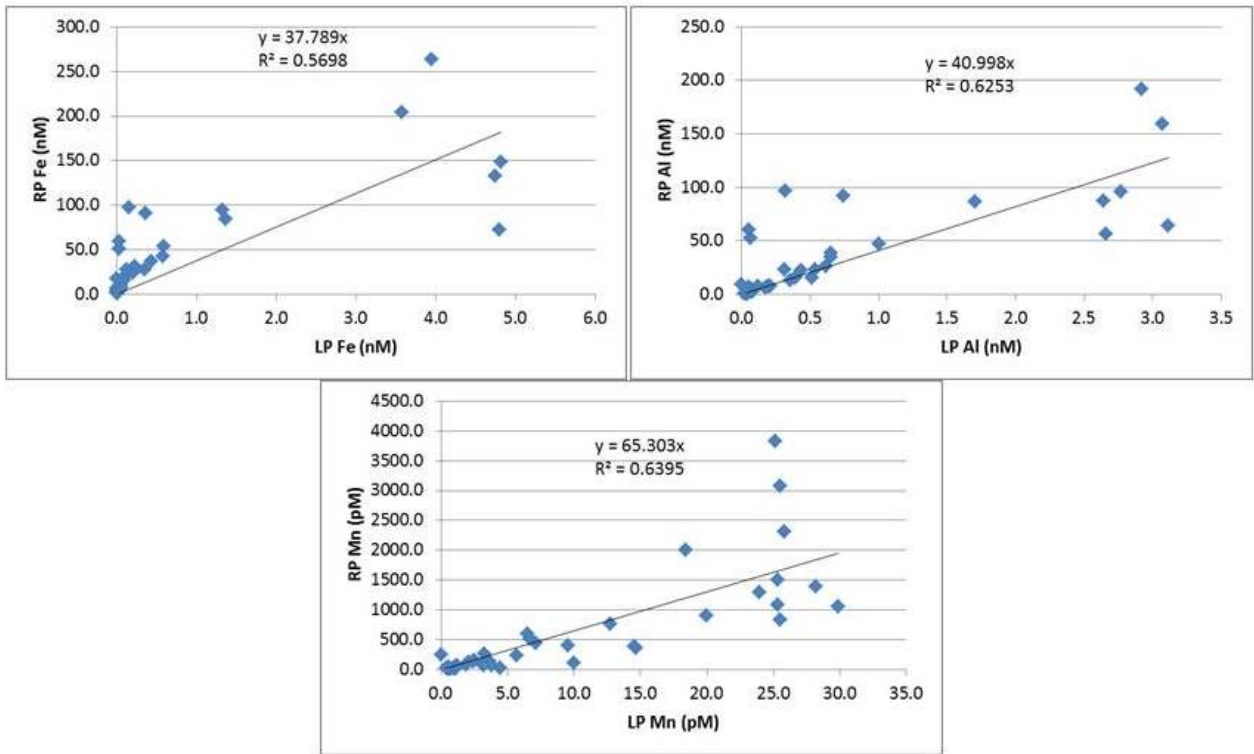
145 **Table S2: Fe, Mn, and Al concentrations in pore waters and sediments**

Date	Station	Sample ID	Sample mid-depth (cm)	Sediment particles			Porewater	
				Fe (wt %)	Mn (ppm)	Al (wt%)	Fe ( $\mu$ mol kg <sup>-1</sup> )	Mn ( $\mu$ mol kg <sup>-1</sup> )
Feb. 2011	S1 (MC33)	AC1	0.5	3.25	635	4.77	3.0	2.421
		AC2	1.5	3.38	633	4.70	17.2	0.940
		AC3	2.5	3.31	647	4.78	110.1	0.546
		AC4	3.5	3.35	662	5.01	105.6	0.675
		AC5	4.5	3.22	649	4.65	93.5	0.520
		AC6	5.5	3.30	662	5.02	81.9	0.389
		AD1	7	-	-	-	52.6	0.271
		AD2	9	3.11	615	4.66	32.6	0.263
		AD3	11	-	-	-	27.3	0.304
		AD4	13	-	-	-	6.4	0.293
		AD5	15	3.09	612	4.69	2.5	0.209
		AD6	17	-	-	-	1.4	0.087
		AE1	19	-	-	-	0.8	0.040
		AE2	21	-	-	-	0.8	0.027
AE3	23	-	-	-	0.7	0.028		
AE4	25	2.99	594	4.31	0.7	0.008		
Feb. 2011	S2 (MC34)	AF1	0.5	3.58	627	4.77	1.5	0.585
		AF2	1.5	3.35	644	4.83	-	-
		AF3	2.5	3.24	649	4.74	1.1	0.399

		AF5	4.5	-	-	-	18.5	0.304
		AG1	6.5	3.32	672	4.94	11.1	0.264
		AG3	8.5	-	-	-	4.7	0.253
		AG5	10.5	3.24	647	4.85	14.5	0.285
		AH1	12.5	-	-	-	3.9	0.290
		AH3	14.5	3.02	595	4.32	3.8	0.285
		AH5	16.5	3.11	616	4.65	2.6	0.336
Feb. 2011	S3 (MC35)	AI1	0.5	3.43	627	4.49	1.6	0.597
		AI2	1.5	3.28	643	4.75	29.0	0.465
		AI3	2.5	3.24	642	4.75	91.1	0.373
		AI4	3.5	3.32	661	4.88	40.2	0.342
		AI5	4.5	-	-	-	37.1	0.262
		AI6	5.5	3.16	636	4.81	49.3	0.535
		AJ1	6.5	-	-	-	37.4	0.251
		AJ2	7.5	-	-	-	61.7	0.322
		AJ3	8.5	3.27	640	4.92	67.9	0.475
		AJ4	11.0	-	-	-	48.2	0.398
		AJ5	13.0	-	-	-	23.6	0.336
		AJ6	15.0	-	-	-	33.5	0.648
		AK1	17.0	3.00	593	4.57	3.8	0.181
		AK2	19.0	3.05	597	4.51	1.9	0.075
		AK3	21.0	-	-	-	1.6	0.005
		AK5	25.0	3.08	615	4.77	3.2	0.071
		AK6	27.0	-	-	-	2.9	0.052
		AL1	29.0	3.10	615	4.83	5.6	0.095



147 **Supplementary Figures**

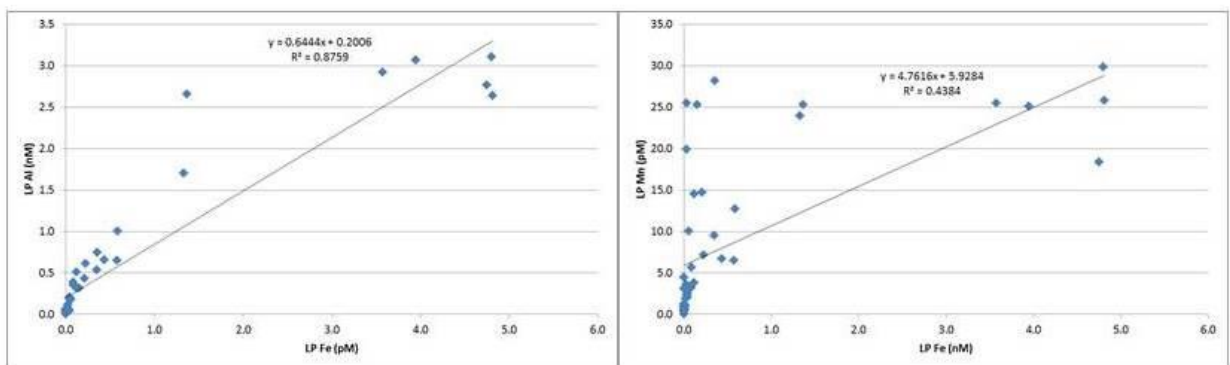


148

149 **Figure S1:** Relationship between leachable particulate (LP) and refractory particulate (RP)

150 Fe, Mn, and Al determined for particulate fraction collected with SAPS.

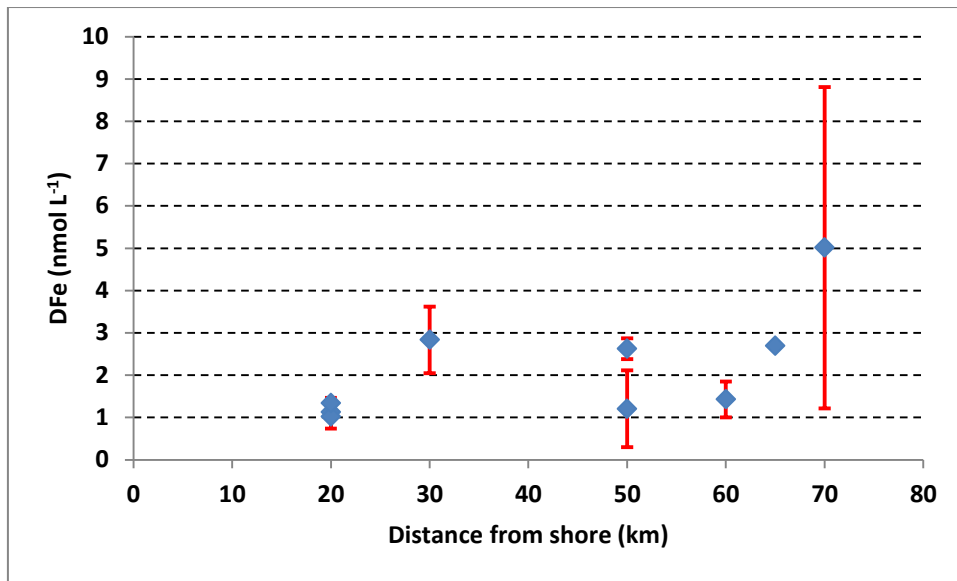
151



152

153 **Figure S2:** Relationship between leachable particulate Fe, Mn and Al.

154



155

156 **Figure S3:** Average dissolved Fe concentration between 100 and 400 m water depth versus

157 distance to the coast line of South Georgia in kilometre.

158 **References**

- 159 Boudreau, B. P. and Scott, M. R.: A model for the diffusion-controlled growth of deep-sea  
160 manganese nodules, *Americ. J. Sc.*, 278, 903-929, 1978.
- 161 de Jong, J., Schoemann, V., Lannuzel, D., Croot, P., de Baar, H. J. W., and Tison, J. L.:  
162 Natural iron fertilization of the Atlantic sector of the Southern Ocean by continental shelf  
163 sources of the Antarctic Peninsula, *J. Geophys. Res.*, 117, 1-25, 2012.
- 164 Ho, T.-Y., Quigg, A., Finkel, Z. V., Milligan, A. J., Wyman, K., Falkowski, P. G., and Morel,  
165 F. M. M.: The elemental composition of some marine phytoplankton, *J. Phycol.*, 39, 1145-  
166 1159, 2003.
- 167 Homoky, W. B., John, S. G., Conway, T. M., and Mills, R. A.: Distinct iron supply and  
168 isotope signatures from marine sediment dissolution, *Nat. Commun.*, 4:2143, 2013.
- 169 Homoky, W. B., Severmann, S., McManus, J., Berelson, W. M., Riedel, T. E., Statham, P. J.,  
170 and Mills, R. A.: Dissolved oxygen and suspended particles regulate the benthic flux of iron  
171 from continental margins, *Mar. Chem.*, 134–135, 59-70, 2012.
- 172 John, S. G., Mendez, J., Moffett, J. W., and Adkins, J.: The flux of iron and iron isotopes  
173 from San Pedro Basin sediments, *Geochim. Cosmochim. Act.*, 93, 14-29, 2012.
- 174 Kagaya, S., Maebe, E., Inoue, Y., Kamichatani, W., Kajiwara, T., Yanai, H., Saito, M., and  
175 Tohda, K.: A solid phase extraction using a chelate resin immobilizing carboxymethylated  
176 pentaethylenehexamine for separation and preconcentration of trace elements in water  
177 samples, *Talanta*, 79, 146-152, 2009.
- 178 Ma, S., Tao, Z., Yang, X., Yu, Y., Zhou, X., M, W., and Li, Z.: Estimation of marine primary  
179 productivity from satellite-derived phytoplankton absorption data, *IEEE J-STARS*, 7, 3084-  
180 3092, 2014.

181 McManus, J., Berelson, W. M., Severmann, S., Johnson, K. S., Hammond, D. E., Roy, M.,  
182 and Coale, K. H.: Benthic manganese fluxes along the Oregon-California continental shelf  
183 and slope, *Cont. Shelf Res.*, 43, 71-85, 2012.

184 Millero, F. J., Sotolongo, S., and Izaguirre, M.: The oxidation kinetics of Fe(II) in seawater,  
185 *Geochim. Cosmochim. Act.*, 51, 793-801, 1987.

186 Raiswell, R. and Anderson, T. F.: Reactive iron enrichment in sediments deposited beneath  
187 euxinic bottom waters: constraints on supply by shelf recycling, Geological Society, London,  
188 Special Publications, 2005.

189 Rapp, I., Schlosser, C., Rusiecka, D., Gledhill, M., and Achterberg, E. P.: Automated  
190 preconcentration of Fe, Zn, Cu, Ni, Cd, Pb, Co, and Mn in seawater with analysis using high-  
191 resolution sector field inductively-coupled plasma mass spectrometry, *Anal. Chimi. Acta*,  
192 976, 1-13, 2017.

193 Strzepek, R., Maldonado, M. T., Hunter, K. A., Frew, R. D., and Boyd, P. W.: Adaptive  
194 strategies by Southern Ocean phytoplankton to lessen iron limitation: Uptake of organically  
195 complexed iron and reduced cellular iron requirements, *Limnol. Oceanogr.*, 56, 1983-2002,  
196 2011.

197 Twining, B. S., Baines, S. B., Fisher, N. S., and Landry, M. R.: Cellular iron contents of  
198 plankton during the Southern Ocean Iron Experiment (SOFeX), *Deep-Sea Res. I*, 51, 1827-  
199 1850, 2004.

200